ACS Sustainable Chemistry & Engineering

Research Article

Cite This: ACS Sustainable Chem. Eng. 2018, 6, 16867−16875

pubs.acs.org/journal/ascecg

# Tuning Hydrocarbon Pool Intermediates by the Acidity of SAPO-34 Catalysts for Improving Methanol-to-Olefins Reaction

Qingqing Peng,[†] Guitao Wang,[†] Zichun Wang,*[,‡] Rongli Jiang,[†] Dan Wang,[§] Jianfeng Chen,[§] and Jun Huang*[,†,‡]

[†]School of Chemical Engineering & Technology, China University Mining & Technology, Xuzhou 221116, People's Republic of China

[‡]Laboratory for Catalysis Engineering, School of Chemical and Biomolecular Engineering, The University of Sydney, Darlington, New South Wales 2006, Australia

[§]State Key Laboratory of Organic−Inorganic Composites, Beijing University of Chemical Technology, North Third Ring Road 15, Chaoyang District, Beijing 100029, People's Republic of China

Supporting Information

**ABSTRACT:** Methanol-to-olefins (MTO) has received great attention, in which abundant renewable resources of biomass and biogas can be utilized as promising alternatives to crude oil in the production of light olefins. SAPO-34 is one of the most promising catalysts in MTO reaction, providing excellent selectivity toward ethylene and propylene. In this work, highly crystalline SAPO-34 catalysts with different $SiO_2/Al_2O_3$ ratios have been applied in MTO reaction to elucidate the effects of particle size and acidity on the "hydrocarbon pool" intermediate distribution, which remarkably influence their catalytic performance in the reaction. A smaller particle size of SAPO-34 catalyst (e.g., 120−360 mesh) can improve the catalyst lifetime, but nearly no effect on the product distribution. A suitable density of Brønsted acid sites (BAS) was found to effectively prolong the catalyst lifetime and enhance the total selectivity toward light olefins (ethylene and propylene). GC−MS and NMR analysis demonstrates that the suitable BAS density on SAPO-34 can suppress hydrogen transfer reaction for the formation of paraffins and the formation of polycyclic aromatics. The suitable BAS density was found to promote the formation of active "hydrocarbon pool" species, such as polymethylbenzenes, at a very low aromatic/$CH_3$ ratio compared to those having a much higher BAS density (>0.2), which can significantly boost the selectivities to olefins as desired products and improve the catalyst lifetime at 100% conversion of methanol. Therefore, this work provides a potential way for the development of suitable catalysts for MTO reaction with high olefin selectivity and improved lifetime.

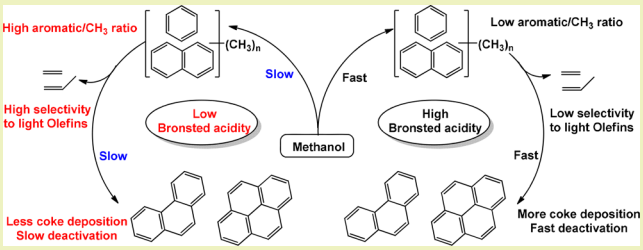


**KEYWORDS:** *Methanol-to-olefin reaction, SAPO-34, Brønsted acidity, Reaction mechanism*

## INTRODUCTION

The increasing demand of light olefins and the constraints of crude oil drive the rapid development of the methanol-to-olefins (MTO) process.[1−4] The MTO process is a nonoil-based reaction discovered by Mobil in the 1970s. It can produce light olefins from abundant resources of coal as well as renewable resources of biomass and biogas as a promising alternative to crude oil, and thus, has received great attentions industrially. SAPO-34, as one of the most promising catalysts in the MTO reaction, exhibits an excellent selectivity toward ethylene and propylene of ca. 80% under the optimized reaction conditions.[4−8] This is owing to the moderate acid strength and chabazite cages (0.67 nm × 1 nm) associated with suitable pore size (8-ring windows (0.38 nm × 0.38 nm)) of SAPO-34 catalyst, which can restrain the conversion of light olefins to alkanes and the formation of olefins with large molecular size. The "hydrocarbon pool" mechanism has been widely accepted for the MTO reaction.[9−11] "Hydrocarbon pool" species have been identified as carbenium ions[12−16] (e.g., heptaMB$^+$ and pentaMCP$^+$ ions) and polymethylbenzenes (PMBs).[11,17−26] During the MTO reaction, methanol or dimethyl ether (DME) is added to PMBs, followed by splitting to generate light olefins as shown in Scheme 1. Improving the selectivity to light olefins and stability of SAPO-34 catalysts in the MTO process is of great importance for their industrial applications.[17−19] Extensive efforts have been devoted to address these issues, such as optimizing the operating conditions,[27] modifying the zeolite pore structure,[28] adjusting the acidity,[29,30] controlling the catalyst morphology and size.[31−34]

Tuning the surface acidity of the SAPO-34 catalyst is a key factor to determine the catalyst stability and the selectivity to

Received: August 23, 2018
Revised: October 24, 2018
Published: November 9, 2018






DOI: 10.1021/acssuschemeng.8b04210
ACS Sustainable Chem. Eng. 2018, 6, 16867−16875

**Scheme 1. Possible Reaction Process of Methanol Conversion over SAPO-34.**

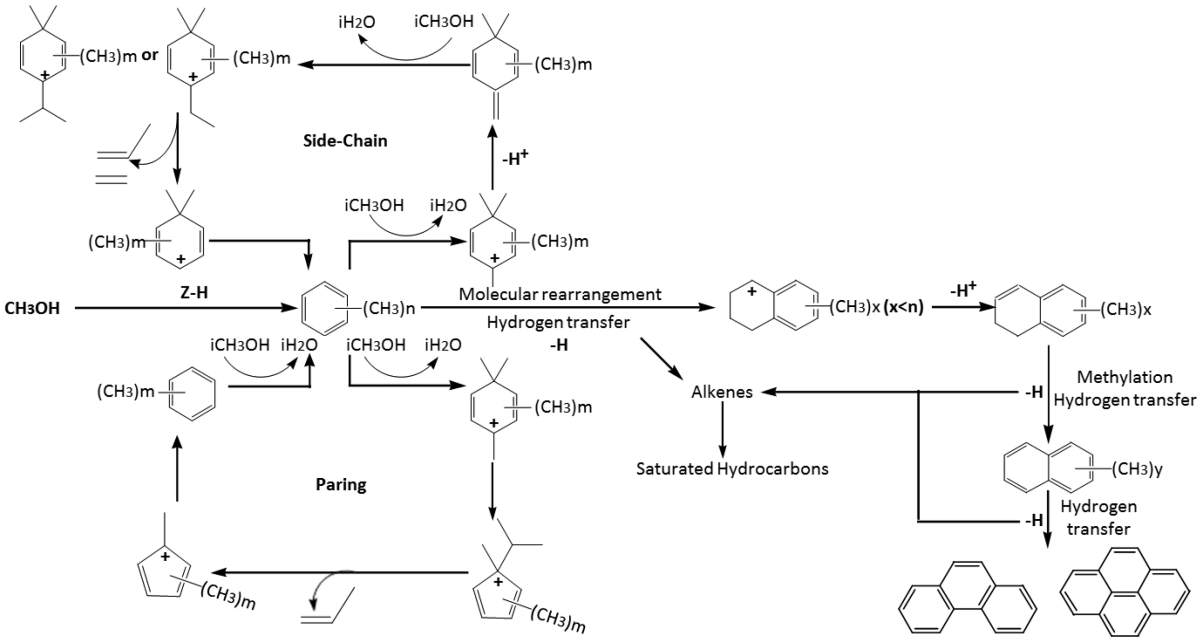


light olefins in the MTO reaction. The surface acid sites are generated from hydrogen atoms bonded to the oxygen atoms in bridging OH groups which are introduced by Si atoms substituting the framework atoms in the neutral AlPO-34.[34−40] Two different Si isomorphous substitution mechanisms have been proposed: (1) SM II, the substitution of P by Si; and (2) SM III, the substitution of adjacent Al and P by two Si atoms. In SM II, the substitution of $P^{5+}$ by $Si^{4+}$ results in a negative charged framework oxygen, which can be compensated by a proton, acting as a catalytically active Brønsted acid site (BAS). While the introduction of Si by only SM III mechanism would form Si−O−P linkages, which is energetically unfavorable.[40] Generally, isolated $Si(OAl)_4$ species are formed by only SM II mechanism at a Si content lower than a threshold value,[41,42] while SM II and SM III mechanisms act together to form $Si(OAl)_n$ ($n$ = 1, 2, 3) species located at the border of Si islands, and their acid strengths follow the order of $Si(OAl)_4$ < $Si(OAl)_3$ < $Si(OAl)_2$ < $Si(OAl)_1$.[42] The acidity of SAPO-34 catalysts has significant effects on their catalytic performance in the MTO reaction. Zhu et al.[43] synthesized a series of proton-type aluminosilicate H/CHA zeolites with different Si/Al ratios to compare their stability in the MTO reaction, in which they found that a low density of BAS can effectively postpone the coking rate. This is similar to that observed by Wilson and Barger earlier,[44] where they reported that reducing Si content in SAPO-34 could decrease the formation of propane. However, a comprehensive understanding about the intermediate-based reaction mechanism of the MTO reaction over SAPO-34 catalysts is still rare, which is key to improve the performance and stability of SAPO-34 catalysts for industrial applications.

Crystal size is also a crucial factor in determining the catalytic performance in the MTO reaction, especially the catalyst stability. SAPO-34 catalysts with small crystal size have been reported to display a longer catalyst lifetime due to their advantage in the enhancement of mass transfer and diffusion.[29,45,46] Dai et al.[29] applied detailed spectroscopic technology to investigate the stability of SAPO-34 catalysts with different crystal size in the MTO reaction. They found olefinic reaction products associated with a longer residence time inside the cages and pores of the SAPO-34 catalysts with larger crystal size, leading to a shorter catalyst lifetime. However, previous studies predominantly concentrated on the influences of originally synthetic crystal size of SAPO-34 catalysts on the catalytic performance in the MTO reaction, but few investigations on the effect of sieved particle size after compressing and crushing on the MTO catalytic performance have been performed, which is of great importance for their industrial applications.

In the present study, SAPO-34 catalysts with different $SiO_2$/$Al_2O_3$ ratios were synthesized, characterized and served as catalysts for the MTO reaction. The particle size of the SAPO-34 catalysts was well controlled and the entrapped organic deposits on the used SAPO-34 catalysts were analyzed by GC−MS and NMR methods. On the basis of these results, the effects of both the Brønsted acidity on SAPO-34 catalysts and the catalyst particle size on the intermediate distribution are demonstrated, which can significantly influence the selectivities to light olefins and the stability of the catalysts as revealed. Finally, a reaction mechanism was proposed based on the performance of SAPO-34 catalysts in the MTO reaction.

## EXPERIMENTAL METHODS

**Preparation of the SAPO-34 Catalysts.** Aluminum isopropoxide (AIP, 24.7 wt % $Al_2O_3$), *ortho*-phosphoric acid solution (85 wt % $H_3PO_4$) and silica sol (25 wt % $SiO_2$) were used as the sources of aluminum, phosphorus and silicon, respectively. The SAPO-34 catalysts were prepared by a hydrothermal method using tetraethylammonium (TEA) as the template following the procedure described in literature.[29] Briefly, AIP, *ortho*-phosphoric acid solution, and distilled water (1:1:50 by molar ratio) were mixed thoroughly under stirring for 2 h, then the mixture of TEA (AIP/TEA = 1:3 by molar ratio) and silica sol with appropriate concentration was added dropwise, and kept stirring for 6 h at ambient temperature. The resulting gel was transferred into a teflon-lined stainless-steel autoclave for static crystallization at 473 K for 24 h. The solid products were recycled by filtration, washing and drying at 353 K for 12 h. Finally, the as-synthesized SAPO-34 catalysts were calcined in


DOI: 10.1021/acssuschemeng.8b04210
ACS Sustainable Chem. Eng. 2018, 6, 16867−16875

Table 1. ICP Analysis and $NH_3$-TPD Data of SAPO-34 with Different $SiO_2/Al_2O_3$ Ratios

| | | Desorption temperature (K) | | Brønsted acid site density (mmol/g) | | |
|---|---|---|---|---|---|---|
| Samples | $n_{Si}/(n_{Si} + n_{Al} + n_P)$ | Low | High | WAS[a] | SAS (BAS)[a] | Total |
| SAPO-34-0.2 | 0.11 | 502 | 715 | 0.20 | 0.85 | 1.05 |
| SAPO-34-0.4 | 0.13 | 499 | 729 | 0.32 | 1.09 | 1.41 |
| SAPO-34-0.6 | 0.15 | 500 | 732 | 0.44 | 1.15 | 1.59 |
| SAPO-34-0.8 | 0.18 | 491 | 721 | 0.44 | 1.16 | 1.60 |

[a]The densities of weak acid sites (WAS) and BAS were determined from the intensity of the low and high temperature peaks, respectively.

the flowing synthetic air at 873 K for 6 h to remove the template. The nomenclature of SAPO-34 catalysts is denoted as SAPO-34-*x*, where *x* is 0.2, 0.4, 0.6 and 0.8, referring to the $SiO_2/Al_2O_3$ ratios in the starting gels. Prior to investigating the effect of particle size on the catalytic performance in the MTO reaction, the catalyst powder was compressed, crushed and sieved. The obtained particles with different sizes are listed in Table S1 as SAPO-34-*x*-a/b/c/d. For instance, SAPO-34-0.2 with particle size of 20−30 mesh was denoted as SAPO-34-0.2-d.

**Characterization of the SAPO-34 Catalysts.** X-ray powder diffraction (XRD) patterns of the SAPO-34 catalysts were recorded in the range of 5−50° on a Bruker D8 diffractometer equipped with Cu K$\alpha$ radiation ($\lambda$ = 0.154 nm, 35 kV, 40 mA). The morphologies of SAPO-34 catalysts were analyzed on a FEI Quanta 250 scanning electron microscopy (SEM). The acidity of the SAPO-34 catalysts was characterized by temperature-programmed desorption of ammonia ($NH_3$-TPD).[30] The $NH_3$-TPD measurements were performed on a Chem BET TPR/TPD Chemisorption Analyzer, CBT-1, QuantaChrome instruments. Prior to the $NH_3$-TPD measurements, SAPO-34 catalyst (30 mg) was loaded and degassed at 793 K for 1 h under He flow (120 mL/min) to completely remove molecules adsorbed on the samples. Then the sample was saturated in the gas mixture of $NH_3$ and He (8.16%, mol/mol) at 373 K for 30 min, flushed with He gas (120 mL/min) for 30 min. Ammonia desorption was carried out with increasing temperature from 323 to 973 K at a constant heating rate of 10 K/min, and the concentration of desorbed ammonia was obtained by a thermal conductivity detector connected to the TPD system.

**MTO Reaction over the SAPO-34 Catalysts.** The MTO reaction was carried out in a fixed-bed quartz reactor (9 mm i.d.) at atmospheric pressure. Typically, SAPO-34 catalysts (0.25 g) were activated under flowing nitrogen gas at 773 K for 2 h. After cooling to the reaction temperature of 698 K, methanol was injected at a feed rate of 0.3 mL/h, corresponding to the weight hourly space velocity (WHSV) of 1.0 $h^{-1}$. The products were analyzed *in situ* by an online gas chromatograph (Bruker GC-456) equipped with a flame ionization detector and a HP-plot-Q capillary column (30 m × 0.32 mm × 20 $\mu$m). A mixed gas with known mole% of possible gas products was applied as a reference. By analyzing the mixed gas, the response factor of each gas product can be obtained via

$$f_i = \frac{f_{i'}}{f_{i',\mathrm{Propane}}} = \frac{y_i/A_i}{y_{\mathrm{Propane}}/A_{\mathrm{Propane}}} \quad (1)$$

where, $f_i$ and $f_{i'}$ are the relative response factor and the absolute response factor, respectively, $y_i$ and $A_i$ are the mole% and peak area of gas *i* in the reference gas. Based on $f_i$ and the obtained peak area from GC analysis, the selectivity of each gas can be calculated. The methanol conversion and product selectivity were calculated based on the carbon balance of the effluent gas without taking the organic deposits on the catalysts into account.

**Characterization of the Entrapped Organic Deposits on the Used SAPO-34 Catalysts.** The entrapped organic deposits on the used catalysts were extracted according to the procedure reported earlier.[32] Typically, the used catalyst (15 mg) was dissolved in 1.0 mL of 15% HF solution for 30 min to complete dissolution of the framework, followed by the addition of $CH_2Cl_2$ (1.0 mL) to extract the released organic deposits. The organic compounds were analyzed by a gas chromatograph equipped with mass spectrometer detector. The organic deposits entrapped inside the pores and cages of the used SAPO-34 above were also characterized by $^1H$ magic-angle-spinning (MAS) and $^{13}C$ cross-polarization MAS (CP/MAS) NMR spectroscopy. $^1H$ and $^{13}C$ MAS NMR investigations were carried out on a Bruker Avance spectrometer at resonance frequencies of 600.1 and 150.9 MHz with a sample spinning rate of 10 kHz using 4 mm MAS rotors. $^1H$ MAS NMR spectra were recorded after single-pulse $\pi/2$ excitation with a repetition time of 5 s. $^{13}C$ cross-polarization (CP) MAS NMR spectra were recorded with a contact time of 2 ms and a repetition time of 5 s.

## RESULTS AND DISCUSSION

**Characterization of SAPO-34 Catalysts.** As shown in Figure S1, the XRD patterns of all as-synthesized SAPO-34 catalysts with different $SiO_2/Al_2O_3$ ratios exhibit a chabazite (CHA) framework structure with characteristic diffraction peaks at ca. 9.5°, 13°, 16°, 21°, 26° and 31°, typically for SAPO-34 as reported in literature.[29,45] The very weak signal at 7.5° observed with SAPO-34-0.8 could be caused by a very small amount of SAPO-5.[47] The SEM images (Figure S2) demonstrate SAPO-34 catalysts are highly crystalline with a cubical morphology in an average crystal size of ca. 15 $\mu$m. The chemical compositions and BET surface areas of the obtained SAPO-34 catalysts are summarized in Table 1 and Table S2. The surface areas for all samples are similar and typical for SAPO-34 catalysts. The obtained $SiO_2/Al_2O_3$ ratios are higher than the $SiO_2/Al_2O_3$ ratios in the starting gel in the range of 0.2−0.6, while the incorporation of silica may be affected at high silica content (e.g., SAPO-34-0.8), which exhibits the similar trends reported earlier.[48]

TPD profiles of ammonia desorbed from the SAPO-34 catalysts with different $SiO_2/Al_2O_3$ ratios are shown in Figure 1. The low temperature desorption peaks (centered at ca. 498 K) are attributed to ammonia adsorbed on surface hydroxyl groups,[33,34] which affords the weak acidity of SAPO-34 catalysts. The high temperature desorption peaks (centered

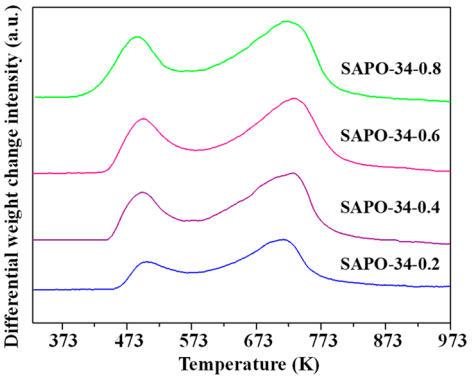


Figure 1. $NH_3$-TPD profiles of SAPO-34 with different $SiO_2/Al_2O_3$ ratios.



DOI: 10.1021/acssuschemeng.8b04210
ACS Sustainable Chem. Eng. 2018, 6, 16867−16875

at ca. 723 K) are assigned to ammonia protonated at the bridging hydroxyl groups (≡Si−OH−Al≡ ), denoted as BAS with moderate Brønsted acid strength.[49] Moreover, the limited change of the high temperature desorption peaks demonstrates that the acid strength of the SAPO-34 catalysts is independent from the silica content. The BAS density of the SAPO-34 catalysts were quantified from the intensity of the desorption peaks and were summarized in Table 1. The BAS density is significantly increased from 1.05 to 1.59 mmol/g with increasing the $n_{Si}/(n_{Si} + n_{Al} + n_P)$ ratio from 0.11 to 0.15, then gradually increased to 1.60 with increasing the $n_{Si}/(n_{Si} + n_{Al} + n_P)$ ratio up to 0.18. The former is attributed to the promotion of BAS formation by $Si^{4+}$ substituting $P^{5+}$ via SMII substitution mechanisms. Because the introduction of Si by only SM III mechanism would form Si−O−P linkages, which is energetically unfavorable,[40] more silicon islands can be formed in the silica framework at high silica content,[50] such as $n_{Si}/(n_{Si} + n_{Al} + n_P) = 0.18$, which may result in that the silicon content determined by chemical analysis (Table S2) is higher than the number of bridging hydroxyls determined by $NH_3$-TPD. Thus, increasing the $SiO_2/Al_2O_3$ ratio has slightly effect on acid strength of SAPO-34, but does increase the BAS density, in a good agreement with previous study.[49]

**Size-Dependent Effect on SAPO-34 Performance in the MTO Reaction.** The MTO reaction was carried out over SAPO-34 catalysts with different particle sizes. The methanol conversion as a function of time on stream (TOS) over SAPO-34-0.2 is plotted in Figure 2. SAPO-34-0.2-b with the particle

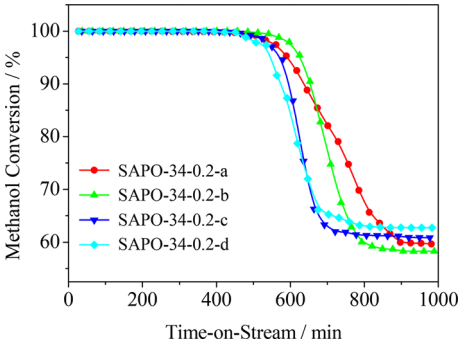


**Figure 2.** Methanol conversion during the MTO reaction over SAPO-34-0.2 catalysts with different particle sizes. Conditions: SAPO-34 catalysts (0.25 g) were loaded and activated in a fixed-bed quartz reactor under flowing nitrogen gas at 773 K for 2 h. Reaction was carried out at 698 K with a methanol feeding rate of 0.3 mL/h and corresponding WHSV of 1.0 $h^{-1}$.

size of 120−360 mesh exhibits the longest catalyst lifetime, which retained a methanol conversion of 100% for 457 min. Increasing the particle size reduced the catalyst lifetime, for example, SAPO-34-0.2-d with the largest particle size of 20−30 mesh retained a methanol conversion of 100% for only 366 min. SAPO-34-0.2-a with the smallest particle size provides a similar lifetime to SAPO-34-0.2-b, but its activity loss is much slower. This may be related to the maldistribution of methanol feed in the compact SAPO-34-0.2-a catalyst bed. Further increasing the particle size of SAPO-34-0.2-c and SAPO-34-0.2-d resulted in a faster activity loss, in comparison with SAPO-34−0.2-b. It indicates smaller particle size is essential to improve the stability of SAPO-34 catalysts in the MTO reaction. This has been further evidenced by the catalytic data obtained with SAPO-34-0.2 at methanol conversion of 70% as shown in Figure 3, where SAPO-34-0.2-a with the smallest particle size exhibits the highest stability, maintaining methanol conversion above 70% for 780 min on stream.

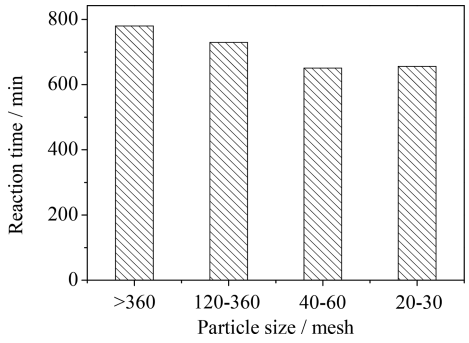


**Figure 3.** Reaction time of SAPO-34-0.2 catalysts from the beginning to 70% methanol conversion.

Notably, all SAPO-34-0.2 catalysts with different particle size are highly selective to ethylene and propylene at the major products in MTO reaction, as summarized in Table 2. The

**Table 2. Products Selectivity of SAPO-34 Catalysts with Different Particle Sizes during the Reaction Period of MTO Reaction at 698 K with a Methanol Feeding Rate of 0.3 mL/h and Corresponding WHSV of 1.0 $h^{-1}$**

| Samples | Ethylene | Propylene | Ethane | Propane |
|---|---|---|---|---|
| SAPO-34-0.2-a | 40.08 | 46.20 | 0.14 | 0.75 |
| SAPO-34-0.2-b | 40.98 | 46.58 | 0.14 | 0.72 |
| SAPO-34-0.2-c | 41.18 | 45.18 | 0.18 | 0.96 |
| SAPO-34-0.2-d | 40.51 | 45.56 | 0.13 | 0.67 |

total selectivity toward olefins are all within the range of 86.07−87.56%, which is independent from the sieved particle size under study. Interestingly, the selectivities toward ethane and propane were below 0.18% and 0.96%, respectively, over all SAPO-34-0.2 catalysts. These alkanes are the main byproducts stemming from the corresponding olefin products by hydrogen transfer reaction. The very low selectivity of alkanes indicates that the hydrogen transfer reaction is suppressed, which is attributed to the low BAS density of SAPO-34-0.2 catalysts and worthy for further discussion.

**Catalytic Performance of SAPO-34 Catalysts with Different $SiO_2/Al_2O_3$ Ratios.** The effect of acidity on the catalytic performance of SAPO-34 in MTO reaction was investigated with the SAPO-34 catalysts with different $SiO_2/Al_2O_3$ ratios. The methanol conversion as a function of TOS at 698 K is presented in Figure 4. The catalyst lifetime obtained at 100% methanol conversion over SAPO-34 catalysts are 351 min for SAPO-34-0.2, 287 min for SAPO-34-0.4, 245 min for SAPO-34-0.6 and 173 min for SAPO-34-0.8. Obviously, the catalyst lifetime was significantly improved by two times with decreasing the $SiO_2/Al_2O_3$ ratio from 0.8 to 0.2. Based on $NH_3$-TPD analysis, the catalyst lifetime remarkably depends on the BAS density adjusted by tuning the $SiO_2/Al_2O_3$ ratios of SAPO-34 catalysts. The decrease of BAS density in SAPO-34 catalysts is in the reverse order of the increase of catalyst lifetime, such as SAPO-34-0.8 < SAPO-34-0.6 < SAPO-34-0.4 < SAPO-34−0.2. With similar BAS density, SAPO-34-0.6 exhibits 40% longer lifetime than SAPO-34-0.8, which could be caused by the slightly enhanced BAS strength as revealed by


DOI: 10.1021/acssuschemeng.8b04210
ACS Sustainable Chem. Eng. 2018, 6, 16867−16875

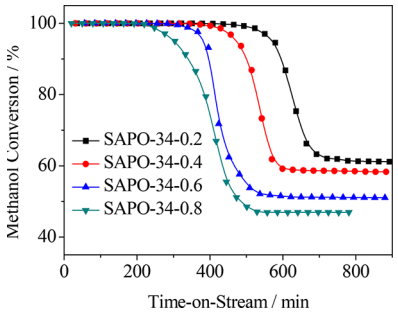


**Figure 4.** Methanol conversion during the MTO reaction over SAPO-34 catalysts with different $SiO_2/Al_2O_3$ ratios at 698 K.

the lower desorption temperature in $NH_3$-TPD analysis (732 K vs 721 K), since the higher acid strength can decrease the energy barrier to promote the reaction.

The products distribution in MTO reaction over SAPO-34 catalysts was studied as a function of $SiO_2/Al_2O_3$ ratios (Figure 5). All SAPO-34 catalysts are highly selective toward light

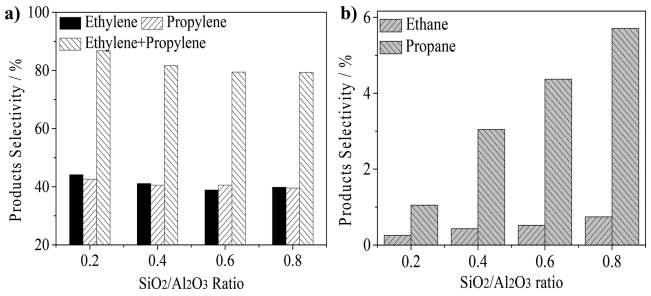


**Figure 5.** Products distribution in MTO reaction over SAPO-34 catalysts with different $SiO_2/Al_2O_3$ ratios at 698 K. (a) Selectivity toward light olefins, (b) Selectivity toward light alkanes.

olefins (e.g., ethylene and propylene) with selectivities over 80%, which was enhanced with lowering the $SiO_2/Al_2O_3$ ratio (Figure 5a). Among them, SAPO-34-0.2 obtained the highest ethylene and propylene selectivity of ca. 44.2% and 42.6%, respectively. Moreover, SAPO-34-0.2, with the lowest $SiO_2/Al_2O_3$ ratio and BAS density, was still active for almost 750 min on stream before ethylene selectivity drops to 5%, compared to 570, 500 and 460 min on stream for SAPO-34-0.4, SAPO-34-0.6 and SAPO-34-0.8, respectively. On the other hand, the total selectivity toward light alkane (e.g., ethane and propane) over SAPO-34 catalysts are all below 6%, which is decreased with increasing $SiO_2/Al_2O_3$ ratio (Figure 5b).

The formation of light alkanes in MTO reaction is induced by intermolecular hydrogen transfer, in which the hydrogen atoms abstracted from the hydrogen donors is transferred to the surface alkoxide group, leading to the formation of aromatics and alkane.[11] Therefore, the selectivity to light alkanes can be used to evaluate the hydrogen transfer level in the same extent. As shown in Figure 5b, the formation rate of ethane is 4.2−8.4 times slower than propane over the SAPO-34 catalysts, respectively, which indicates that propene is a facile hydrogen acceptor compared with ethane. This is reasonable because the reactivity of olefins is closely related to the degree of substitution about the double bond. The lowest light alkane selectivity (1.3%) obtained with SAPO-34-0.2, followed by SAPO-34-0.4 (3.5%), SAPO-34-0.6 (4.9%) and SAPO-34-0.8 (6.5%), indicating the hydrogen transfer can be suppressed with decreasing BAS density over SAPO-34, in consistent with that reported earlier.[44] Furthermore, the low alkane selectivity over SAPO-34-0.2 is in line with the slow coking rate. Therefore, the present work clearly demonstrates a lower BAS density with reducing $SiO_2/Al_2O_3$ ratio can not only improve the lifetime of SAPO-34 catalysts, but also enhance the selectivity toward light olefins and suppress the light alkanes as byproduct.

**Entrapped Organic Deposits on SAPO-34 Catalysts Investigated by GC−MS Analysis.** The entrapped organic deposits on the SAPO-34-0.2 and SAPO-34-0.6 catalysts during the reaction period and deactivation period were investigated by GC−MS chromatograms (Figure 6a,b),

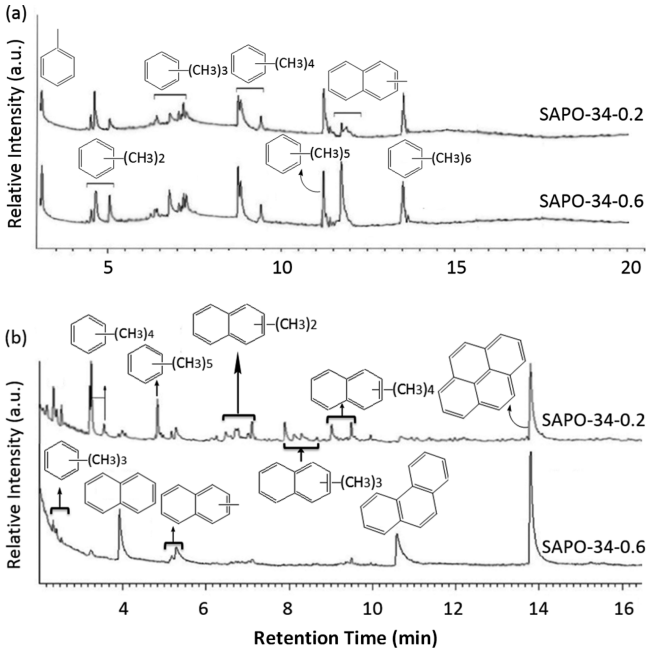


**Figure 6.** GC−MS chromatograms of entrapped organic deposits on the used SAPO-34-0.2 and SAPO-34-0.6 catalysts: (a) reaction period; (b) deactivation period.

respectively. As shown in Figure 6a, similar organic compositions consisting of PMBs and polymethylnaphthalenes (PMNs) were detected. The amount of methylbenzenes with 4−6 methyl groups is much larger than those with 1−3 methyl groups, suggesting that higher methylbenzenes are predominant on the SAPO-34 catalysts during the reaction period particularly on SAPO-43-0.2. A distinct higher amount of PMNs was probed on SAPO-34-0.6 than on SAPO-43-0.2. As shown in Scheme 2, the amount of PMBs and PMNs accounts for ca. 93.03% and ca. 6.97% on SAPO-34-0.2, respectively, while the amount of PMBs decreases to ca. 76.1% and the amount of PMNs increases to ca. 23.9% on SAPO-34-0.6.

On the deactivated SAPO-34-0.2 and SAPO-34-0.6 catalysts (Figure 6b), the residue consists of mainly bi- and polycyclic aromatic compounds, instead of PMBs and PMNs on nondeactivated catalysts (Figure 6a). The surface of deactivated SAPO-34-0.6 is dominated by naphthalene, phenanthrene and pyrene species, while appreciable amounts of PMBs, MNs having 2−4 methyl groups are the main aromatic compounds on deactivated SAPO-34-0.2, which contains tiny amounts of naphthalene, phenanthrene and relative low content of pyrene compared to SAPO-34-0.6. As


DOI: 10.1021/acssuschemeng.8b04210
ACS Sustainable Chem. Eng. 2018, 6, 16867−16875

**Scheme 2. Content of the Aromatics and Deactivation Mechanism on SAPO-34 Catalysts**

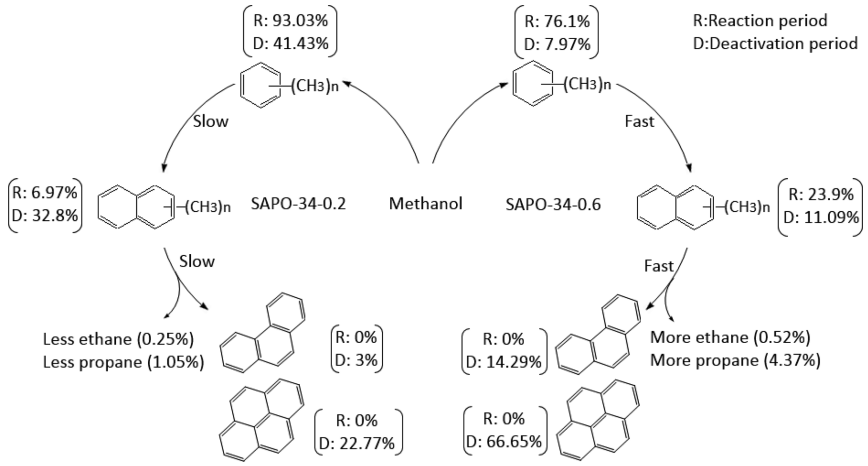


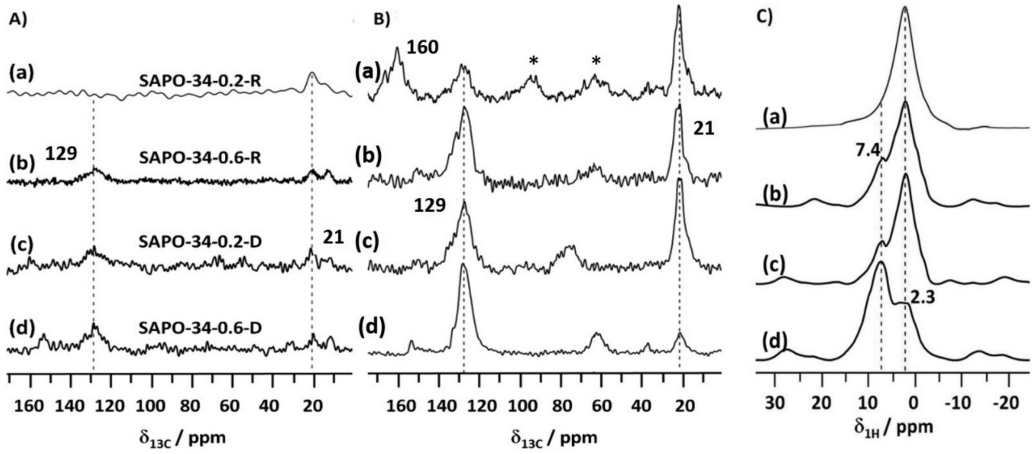


**Figure 7.** NMR spectra of the entrapped organic deposits on the used SAPO-34 catalysts: (A) $^{13}$C HPDEC NMR, (B) $^{13}$C CP MAS NMR, (C) $^{1}$H MAS NMR. In each figure, (a) and (b) indicate the catalysts obtained during the reaction period, and (c) and (d) from the deactivation period. * represents sideband in the spectra.

shown in Scheme 2, the amounts of PMBs, PMNs, phenanthrene and pyrene account for ca. 41.43%, 32.8%, 3% and 22.77% of the total aromatics on SAPO-34-0.2, respectively. On SAPO-34-0.6, the amounts of PMBs and PMNs decrease to ca. 7.97% and 11.09%, respectively, while the amounts of phenanthrene and pyrene increase to ca. 14.29% and 66.65%, respectively. The polycyclic aromatics could be generated by the hydrogen transfer between primary olefins and the hydrocarbon pool compounds (e.g., PMBs and PMNs). Therefore, the low BAS density on SAPO-34-0.2 seems to hamper the hydrogen transfer reaction, and thus, slow down the evolution of the PMBs to the polycyclic aromatics, which prolong the catalyst lifetime.

**Entrapped Organic Deposits on SAPO-34 Catalysts Studied by Solid State NMR.** Direct polarization and cross-polarization $^{13}$C solid state MAS NMR spectroscopy were applied in the study of the entrapped organic deposits on the used SAPO-34 catalysts during the reaction period and deactivation period are shown in Figure 7A,B, and a survey on the assignments of $^{13}$C MAS NMR signals occurring in the used SAPO-34 catalysts from literature is given in Table S2.[51] The signals at $\delta_{13C}$ = 129 and 21 ppm are assigned to aromatic carbon atoms and the methyl carbon atoms bound to aromatic rings. These assignments are confirmed by $^{1}$H MAS NMR investigations (Figure 7C), where the $\delta_{1H}$ = 7.4 and 2.3 ppm are caused by the hydrogen atoms bound to aromatic rings and in methyl groups connected with aromatic rings (e.g., hydrogen atoms in toluene), respectively. In $^{1}$H−$^{13}$C CP MAS NMR experiment (Figure 7B), the polarization is transferred from protons to the dipolarly coupled carbon, which can remarkably enhance the signal of carbon atoms coupled with neighboring protons. By comparing the spectra in Figure 7A with corresponding CP MAS NMR spectra in Figure 7B, the methyl carbon signal $\delta_{13C}$ = 21 ppm was enhanced dramatically, accompanied with the signal at $\delta_{13C}$ = 129 ppm. Their dominant role demonstrates polymethylaromatics are the major organic deposits on both the SAPO-34 catalysts obtained during the reaction period. By normalizing the methyl carbon signals in parts (a) and (b) in Figure 7B, the relative strong signal at $\delta_{13C}$ = 129 ppm on SAPO-34-0.6 indicates more PMNs were formed than on SAPO-34-0.2, in line with GC−MS analysis.

During the deactivation period, the signals at $\delta_{13C}$ = 129 ppm in parts (c) and (d) in Figure 7A,B are remarkably increased, compared with their corresponding spectra under reaction conditions. This indicates more aromatic carbon was formed. The higher ratio between the signal intensity of aromatic carbon and the signal intensity of methyl carbon than those at reaction conditions (Figure 7B(c),(d) indicates the polymerization of aromatic rings. Particularly, only a very weak



DOI: 10.1021/acssuschemeng.8b04210
ACS Sustainable Chem. Eng. 2018, 6, 16867−16875

**Scheme 3. Hydrocarbon Intermediates on SAPO-34 with Different $SiO_2/Al_2O_3$ Ratios in MTO Reaction**

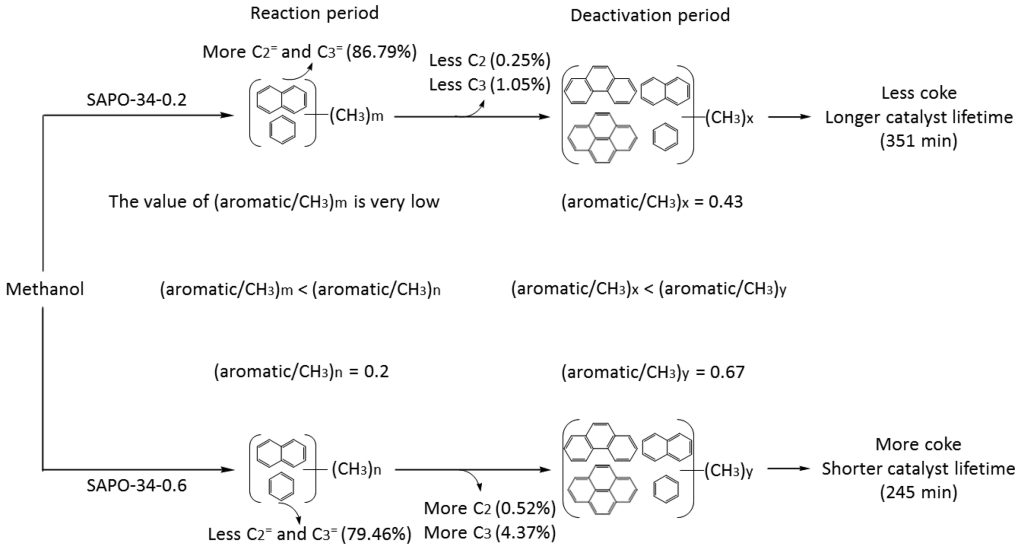


methyl carbon signal can be observed in Figure 7B(d), as well as the aromatic hydrogen dominates in Figure 7C(d). In the meanwhile, methyl groups plays a dominant role on SAPO-34−0.2 with a relative weak signal of aromatic carbon (Figure 7C(c)). Obviously, polycyclic aromatic hydrocarbons were the dominant carbon species on the deactivated SAPO-34 surface, while the surface of SAPO-34-0.2 was dominated with a relative higher content of polymethylaromatics than those on SAPO-34-0.6 surface, in agreement with GC−MS analysis. This indicates more BAS was in favor of the formation aromatic compounds and consumes a large amount of methyl groups in the side chain, which lowers the catalyst stability.

**Discussion of Reaction Mechanism over SAPO-34 Catalysts.** The different reaction process of methanol conversion over SAPO-34 with different $SiO_2/Al_2O_3$ ratios were summarized in Scheme 3, along with the corresponding aromatic/$CH_3$ ratios. The aromatic/$CH_3$ ratios were obtained from $^{13}C$ HPDEC MAS NMR:

$$\text{Aromatic to } CH_3 \text{ ratio} = \frac{\text{The area of 129 ppm/6}}{\text{The area of 21 ppm/1}}, \text{ all areas from Figure 7A} \quad (2)$$

In the reaction period, the aromatic/$CH_3$ ratio obtained with SAPO-34-0.6 was 0.2, much larger than that obtained with SAPO-34-0.2. Similarly, in the deactivation period, the aromatic/$CH_3$ ratio obtained with SAPO-34-0.6 was 0.67, compared to 0.43 obtained with SAPO-34-0.2. Based on $NH_3$-TPD analysis coupled with catalytic test, it exhibits a reverse order between the BAS density and catalyst lifetime of SAPO-34. It may demonstrate that less BAS was conducive to decrease the cost of methyl groups and accelerate the formation of aromatics.

During MTO reactions, aromatics can be formed over BAS through bimolecular reactions, such as hydrogen transfer, as well as via molecular rearrangement as shown in Scheme 1. With a low BAS density, these reactions can be depressed over SAPO-34-0.2, resulting in a very low aromatic/$CH_3$ ratio during the reaction period. This demonstrates the MTO reaction over SAPO-34-0.2 may proceed through an alkene cycle, such as to produce ethylene and propylene via the dehydration of dimethyl ether that obtained from methanol dehydration. Over SAPO-34-0.6, the higher number of BAS can facilitate the formation of PMBs, much higher than those generated on SAPO-34-0.2 (Figure 6a). PMBs, acting as the active intermediates, react with methanol to generate the lower olefins through side-chain (Scheme S1) and paring (Scheme S2) alkylation routes over SAPO-34-0.6, which are also possible over SAPO-34-0.2 after the formation of PMBs.

With MTO reaction proceeding, PMNs and polycyclic aromatics are the dominant species on deactivated SAPO-34 catalysts (Figure 6b). PMNs were generated through molecular rearrangement and hydrogen transfer reactions.[20] Subsequently, the aging of PMBs and PMNs with the hydrogen transfer reactions between primary olefins and these hydrocarbon pool species leads to the formation of polycyclic aromatics. With more BAS, it promotes the formation of polycyclic aromatics from PMBs and PMNs, and thus, decrease the number of PMBs as the active intermediates for olefin production. Moreover, the higher number of BAS facilitates the aggravation of polycyclic aromatics, which can block these surface active sites. Therefore, a much higher aromatic/$CH_3$ ratio was obtained with SAPO-34-0.6 than with SAPO-34-0.2, leading to a faster deactivation. Meanwhile, the lower number of BAS on SAPO-34-0.2 can depress hydrogen transfer. As shown in Scheme 1, the abstracted hydrogen atoms from the hydrogen donors can be transferred to the primary alkenes to generate saturated hydrocarbons in hydrogen transfer reaction, resulting in ethane and propane. Thus, SAPO-34-0.2 provides a higher selectivity toward ethylene and propylene than SAPO-34-0.6 as shown in Scheme 3.

## CONCLUSIONS

In this work, highly crystalline SAPO-34 catalysts with different $SiO_2/Al_2O_3$ ratios are synthesized for MTO reaction. $NH_3$-TPD analysis shows that the $SiO_2/Al_2O_3$ ratio has little effect on BAS strength, but affects the BAS density. SAPO-34 with particle size exhibits only a slight effect on the selectivities to light olefins (~87%), but can improve the catalyst stability. SAPO-34-0.2 with particle size of 120−360 mesh provides a longer lifetime (457 min) at 100% methanol conversion than that with other particle sizes. Furthermore, SAPO-34-0.2 with


DOI: 10.1021/acssuschemeng.8b04210
ACS Sustainable Chem. Eng. 2018, 6, 16867−16875

the lowest BAS density provides the highest catalyst stability and the highest total selectivity toward ethylene and propylene, compared to other SAPO-34 catalysts with higher $SiO_2/Al_2O_3$ ratios with identical particle size. GC−MS and NMR methods are employed to analyze the nature and amount of organic deposits. During the MTO reaction, the low BAS density of SAPO-34-0.2 can provide a much lower aromatic/$CH_3$ ratio than those obtained over SAPO-34 catalysts with higher BAS densities, exhibiting more PMBs to boost the selectivity to light olefins. In the deactivation period, a lower aromatic/$CH_3$ ratio (0.43 vs 0.67) was obtained with SAPO-34-0.2 as well, which afforded a longer catalyst lifetime (351 min) than others (<287 min) showing a high concentration of polycyclic aromatic deposits. It demonstrates that (1) PMBs are the active "carbon pool" species; (2) the formation of polycyclic aromatics from PMBs via hydrogen transfer reaction over BAS causes the catalyst deactivation; and (3) selectivity toward olefins can be affected by the formation of paraffins via hydrogen transfer reactions. Therefore, a lower BAS density can suppress the hydrogen transfer reaction, which can improve the olefin selectivity and the resistance to catalyst deactivation. Based on these results, the systematic study on the effects of catalyst particle size and acidity on catalyst deactivation and product distribution in this work sheds light on the development of high performance catalysts for MTO reaction.

## ■ ASSOCIATED CONTENT

### Supporting Information

The Supporting Information is available free of charge on the ACS Publications website at DOI: 10.1021/acssuschemeng.8b04210.

XRD patterns and SEM images of SAPO-34 catalysts, tables of catalyst preparation and NMR assignments, proposed reaction schemes for the MTO reaction (PDF)

## ■ AUTHOR INFORMATION


### Corresponding Authors

*J. Huang. E-mail: jun.huang@sydney.edu.au.
*Z. Wang. E-mail: zichun.wang@sydney.edu.au.

### ORCID

Zichun Wang: 0000-0002-4280-2787
Dan Wang: 0000-0002-3515-4590
Jun Huang: 0000-0001-8704-605X


### Notes

The authors declare no competing financial interest.

## ■ ACKNOWLEDGMENTS

J.H. and Z.W. acknowledge the financial supports from Australian Research Council Discovery Projects (DP150103842). J.H. thanks Faculty's Energy & Materials Clusters and MCR scheme and the International Project Development Funding at the University of Sydney. J.H., R.J., Q.P., and G.W. are grateful to the National Natural Science Foundation of China (51674262) for their financial support. J.F. and D.W. acknowledge the funding provided by the National Natural Science Foundation of China (21620102007).

## ■ REFERENCES


(1) Tian, P.; Wei, Y.; Ye, M.; Liu, Z. Methanol to Olefins (MTO): from fundamentals to commercialization. *ACS Catal.* **2015**, *5*, 1922−1938.
(2) Olsbye, U.; Svelle, S.; Bjorgen, M.; Beato, P.; Janssens, T. V. W.; Joensen, F.; Bordiga, S.; Lillerud, K. P. Conversion of methanol to hydrocarbons: how zeolite cavity and pore size controls product selectivity. *Angew. Chem., Int. Ed.* **2012**, *51*, 5810−5831.
(3) Chang, C. D. Hydrocarbons from methanol. *Catal. Rev.: Sci. Eng.* **1983**, *25*, 1−118.
(4) Stöcker, M. Methanol-to-hydrocarbons: catalytic materials and their behavior. *Microporous Mesoporous Mater.* **1999**, *29*, 3−48.
(5) Chen, J. Q.; Bozzano, A.; Glover, B.; Fuglerud, T.; Kvisle, S. Recent advancements in ethylene and propylene production using the UOP/Hydro MTO process. *Catal. Today* **2005**, *106*, 103−107.
(6) Sun, Q.; Xie, Z.; Yu, J. The state-of-the-art synthetic strategies for SAPO-34 zeolite catalysts in methanol-to-olefin conversion. *Natl. Sci. Rev.* **2018**, *5*, 542.
(7) Zhong, J.; Han, J.; Wei, Y.; Tian, P.; Guo, X.; Song, C.; Liu, Z. Recent advances of the nano-hierarchical SAPO-34 in the methanol-to-olefin (MTO) reaction and other applications. *Catal. Sci. Technol.* **2017**, *7*, 4905−4923.
(8) Zhou, Y.; Qi, L.; Wei, Y. X.; Yuan, C. Y.; Zhang, M. Z.; Liu, Z. M. Methanol-to-olefin induction reaction over SAPO-34. *Chin. J. Catal.* **2016**, *37*, 1496−1501.
(9) Wang, W.; Buchholz, A.; Seiler, M.; Hunger, M. Evidence for an initiation of the methanol-to-olefin process by reactive surface methoxy groups on acidic zeolite catalysts. *J. Am. Chem. Soc.* **2003**, *125*, 15260−15267.
(10) Wang, W.; Jiang, Y. J.; Hunger, M. Mechanistic investigations of the methanol-to-olefin (MTO) process on acidic zeolite catalysts by in situ solid-state NMR spectroscopy. *Catal. Today* **2006**, *113*, 102−114.
(11) Dai, W. L.; Wang, C. M.; Dyballa, M.; Wu, G. J.; Guan, N. J.; Li, L. D.; Xie, Z. K.; Hunger, M. Understanding the early stages of the methanol-to-olefin conversion on H-SAPO-34. *ACS Catal.* **2015**, *5*, 317−326.
(12) Xu, S.; Zheng, A.; Wei, Y.; Chen, J.; Li, J.; Chu, Y.; Zhang, M.; Wang, Q.; Zhou, Y.; Wang, J.; Deng, F.; Liu, Z. Direct observation of cyclic carbenium ions and their role in the catalytic cycle of the methanol-to-olefin reaction over chabazite zeolites. *Angew. Chem., Int. Ed.* **2013**, *52*, 11564−11568.
(13) Wang, C.; Chu, Y.; Zheng, A.; Xu, J.; Wang, Q.; Gao, P.; Qi, G.; Gong, Y.; Deng, F. New insight into the hydrocarbon-pool chemistry of the methanol-to-olefins conversion over zeolite H-ZSM-5 from GC-MS, solid-state NMR spectroscopy, and DFT calculations. *Chem. - Eur. J.* **2014**, *20*, 12432−12443.
(14) Xiao, D.; Xu, S.; Han, X.; Bao, X.; Liu, Z.; Blanc, F. Direct structural identification of carbenium ions and investigation of host−guest interaction in the methanol to olefins reaction obtained by multinuclear NMR correlations. *Chem. Sci.* **2017**, *8*, 8309−8314.
(15) Wang, C.; Yi, X.; Xu, J.; Qi, G.; Gao, P.; Wang, W.; Chu, Y.; Wang, Q.; Feng, N.; Liu, X.; Zheng, A.; Deng, F. Experimental evidence on the formation of ethene through carbocations in methanol conversion over H-ZSM-5 zeolite. *Chem. - Eur. J.* **2015**, *21*, 12061−12068.
(16) Wang, C.; Xu, J.; Qi, G.; Gong, Y.; Wang, W.; Gao, P.; Wang, Q.; Feng, N.; Liu, X.; Deng, F. Methylbenzene hydrocarbon pool in methanol-to-olefins conversion over zeolite H-ZSM-5. *J. Catal.* **2015**, *332*, 127−137.
(17) Hereijgers, B. P. C.; Bleken, F.; Nilsen, M. H.; Svelle, S.; Lillerud, K. P.; Bjorgen, M.; Weckhuysen, B. M.; Olsbye, U. Product shape selectivity dominates the methanol-to-olefins (MTO) reaction over H-SAPO-34 catalysts. *J. Catal.* **2009**, *264*, 77−87.
(18) Olsbye, U.; Bjorgen, M.; Svelle, S.; Lillerud, K. P.; Kolboe, S. Mechanistic insight into the methanol-to-hydrocarbons reaction. *Catal. Today* **2005**, *106*, 108−111.
(19) Dai, W. L.; Scheibe, M.; Guan, N. J.; Li, L. D.; Hunger, M. Fate of Brønsted acid sites and benzene-based carbenium ions during



DOI: 10.1021/acssuschemeng.8b04210
*ACS Sustainable Chem. Eng.* 2018, 6, 16867−16875

methanol-to-olefin conversion on SAPO-34. *ChemCatChem* **2011**, *3*, 1130−1133.
(20) Bjorgen, M.; Olsbye, U.; Kolboe, S. Coke precursor formation and zeolite deactivation: mechanistic insights from hexamethylbenzene conversion. *J. Catal.* **2003**, *215*, 30−44.
(21) Dahl, I. M.; Kolboe, S. On the reaction mechanism for hydrocarbon formation from methanol over SAPO-34 0.2. Isotopic labeling studies of the co-reaction of propene and methanol. *J. Catal.* **1996**, *161*, 304−309.
(22) Dahl, I. M.; Kolboe, S. On the reaction-mechanism for hydrocarbon formation from methanol over SAPO-34 0.1. Isotopic labeling studies of the co-reaction of ethene and methanol. *J. Catal.* **1994**, *149*, 458−464.
(23) Mole, T.; Whiteside, J. A.; Seddon, D. Aromatic co-catalysis of methanol conversion over zeolite catalysts. *J. Catal.* **1983**, *82*, 261−266.
(24) Song, W.; Fu, H.; Haw, J. F. Supramolecular origins of product selectivity for methanol-to-olefin catalysis on HSAPO-34. *J. Am. Chem. Soc.* **2001**, *123*, 4749−4754.
(25) Lesthaeghe, D.; De Sterck, B.; Van Speybroeck, V.; Marin, G. B.; Waroquier, M. Zeolite shape-selectivity in the gem-methylation of aromatic hydrocarbons. *Angew. Chem., Int. Ed.* **2007**, *46*, 1311−1314.
(26) Arstad, B.; Nicholas, J. B.; Haw, J. F. Theoretical study of the methylbenzene side-chain hydrocarbon pool mechanism in methanol to olefin catalysis. *J. Am. Chem. Soc.* **2004**, *126*, 2991−3001.
(27) Barger, P. T. Methanol Conversion Process Using SAPO Catalysts. U.S. Patent 5,095,163, 1992.
(28) Park, J. W.; Seo, G. IR study on methanol-to-olefin reaction over zeolites with different pore structures and acidities. *Appl. Catal., A* **2009**, *356*, 180−188.
(29) Dai, W.; Wu, G.; Li, L.; Guan, N.; Hunger, M. Mechanisms of the deactivation of SAPO-34 materials with different crystal sizes applied as MTO catalysts. *ACS Catal.* **2013**, *3*, 588−596.
(30) Izadbakhsh, A.; Farhadi, F.; Khorasheh, F.; Sahebdelfar, S.; Asadi, M.; Feng, Y. Z. Effect of SAPO-34's composition on its physico-chemical properties and deactivation in MTO process. *Appl. Catal., A* **2009**, *364*, 48−56.
(31) Wu, L.; Liu, Z.; Xia, L.; Qiu, M.; Liu, X.; Zhu, H.; Sun, Y. Effect of SAPO-34 molecular sieve morphology on methanol to olefins performance. *Chin. J. Catal.* **2013**, *34*, 1348−1356.
(32) Guisnet, M. Coke" molecules trapped in the micropores of zeolites as active species in hydrocarbon transformations. *J. Mol. Catal. A: Chem.* **2002**, *182*−*183*, 367−382.
(33) Kang, M. Methanol conversion on metal-incorporated SAPO-34s (MeAPSO-34s). *J. Mol. Catal. A: Chem.* **2000**, *160*, 437−444.
(34) Ashtekar, S.; Chilukuri, S. V. V.; Chakrabarty, D. K. Small-pore molecular sieves SAPO-34 and SAPO-44 with chabazite structure: a study of silicon incorporation. *J. Phys. Chem.* **1994**, *98*, 4878−4883.
(35) Sastre, G.; Lewis, D. W.; Catlow, C. R. A. Modeling of silicon substitution in SAPO-5 and SAPO-34 molecular sieves. *J. Phys. Chem. B* **1997**, *101*, 5249−5262.
(36) Vomscheid, R.; Briend, M.; Peltre, M. J.; Man, P. P.; Barthomeuf, D. The role of the template in directing the Si distribution in SAPO zeolites. *J. Phys. Chem.* **1994**, *98*, 9614−9618.
(37) Dumitriu, E.; Azzouz, A.; Hulea, V.; Lutic, D.; Kessler, H. Synthesis, characterization and catalytic activity of SAPO-34 obtained with piperidine as templating agent. *Microporous Mater.* **1997**, *10*, 1−12.
(38) Chakraborty, B.; Pulikottil, A. C.; Viswanathan, B. Physicochemical and MAS NMR characterization of mesoporous SAPOs. *Appl. Catal., A* **1998**, *167*, 173−181.
(39) Prakash, A. M.; Unnikrishnan, S. Synthesis of SAPO-34 - high-silicon incorporation in the presence of morpholine as template. *J. Chem. Soc., Faraday Trans.* **1994**, *90*, 2291−2296.
(40) Suib, S. L.; Winiecki, A. M.; Kostapapas, A. Surface chemical-states of aluminophosphate and silicoaluminophosphate molecular-sieves. *Langmuir* **1987**, *3*, 483−488.
(41) Xu, L.; Du, A. P.; Wei, Y. X.; Wang, Y. L.; Yu, Z. X.; He, Y. L.; Zhang, X. Z.; Liu, Z. M. Synthesis of SAPO-34 with only Si(4Al) species: Effect of Si contents on Si incorporation mechanism and Si coordination environment of SAPO-34. *Microporous Mesoporous Mater.* **2008**, *115*, 332−337.
(42) Barthomeuf, D. Topological model for the compared acidity of SAPOs and SiAl zeolites. *Zeolites* **1994**, *14*, 394−401.
(43) Zhu, Q. J.; Kondo, J. N.; Ohnuma, R.; Kubota, Y.; Yamaguchi, M.; Tatsumi, T. The study of methanol-to-olefin over proton type aluminosilicate CHA zeolites. *Microporous Mesoporous Mater.* **2008**, *112*, 153−161.
(44) Wilson, S.; Barger, P. The characteristics of SAPO-34 which influence the conversion of methanol to light olefins. *Microporous Mesoporous Mater.* **1999**, *29*, 117−126.
(45) Yang, G. J.; Wei, Y. X.; Xu, S. T.; Chen, J. R.; Li, J. Z.; Liu, Z. M.; Yu, J. H.; Xu, R. R. Nanosize-enhanced lifetime of SAPO-34 catalysts in methanol-to-olefin reactions. *J. Phys. Chem. C* **2013**, *117*, 8214−8222.
(46) Chen, D.; Moljord, K.; Fuglerud, T.; Holmen, A. The effect of crystal size of SAPO-34 on the selectivity and deactivation of the MTO reaction. *Microporous Mesoporous Mater.* **1999**, *29*, 191−203.
(47) Xi, D.; Sun, Q.; Chen, X.; Wang, N.; Yu, J. The recyclable synthesis of hierarchical zeolite SAPO-34 with excellent MTO catalytic performance. *Chem. Commun.* **2015**, *51*, 11987−11989.
(48) Liu, G.; Tian, P.; Li, J.; Zhang, D.; Zhou, F.; Liu, Z. Synthesis, characterization and catalytic properties of SAPO-34 synthesized using diethylamine as a template. *Microporous Mesoporous Mater.* **2008**, *111*, 143−149.
(49) Shen, W. L.; Li, X.; Wei, Y. X.; Tian, P.; Deng, F.; Han, X. W.; Bao, X. H. A study of the acidity of SAPO-34 by solid-state NMR spectroscopy. *Microporous Mesoporous Mater.* **2012**, *158*, 19−25.
(50) Zibrowius, B.; Löffler, E.; Hunger, M. Multinuclear MAS NMR and IR spectroscopic study of silicon incorporation into SAPO-5, SAPO-31, and SAPO-34 molecular sieves. *Zeolites* **1992**, *12*, 167−174.
(51) Jiang, Y. J.; Huang, J.; Reddy Marthala, V. R.; Ooi, Y. S.; Weitkamp, J.; Hunger, M. In situ MAS NMR-UV/Vis investigation of H-SAPO-34 catalysts partially coked in the methanol-to-olefin conversion under continuous-flow conditions and of their regeneration. *Microporous Mesoporous Mater.* **2007**, *105*, 132−139.


DOI: 10.1021/acssuschemeng.8b04210
*ACS Sustainable Chem. Eng.* 2018, 6, 16867−16875